



RADIOLOGY—ORIGINAL ARTICLE

Initial human experience with Rubidium-82 renal PET/CT imaging

Abdel K Tahari,¹ Paco E Bravo,¹ Arman Rahmim,¹ Frank M Bengel² and Zsolt Szabo¹

¹Division of Nuclear Medicine, Department of Radiology, Johns Hopkins University School of Medicine, Baltimore, Maryland, USA; and ²Department of Nuclear Medicine, Hannover Medical School, Hannover, Germany

AK Tahari MD, PhD; PE Bravo MD; A Rahmim PhD; FM Bengel MD; Z Szabo MD, PhD.

Correspondence

Dr Abdel K. Tahari, 601 N. Caroline Street, Suite 3223, Baltimore, MD 21287, USA.

Email: atahari1@jhmi.edu

Conflict of interest: No conflict of interest.

Submitted 20 February 2013; accepted 22 April 2013.

doi:10.1111/1754-9485.12079

Abstract

Introduction: Preclinical data have shown that Rubidium-82 chloride (⁸²Rb) is a radiotracer with high first pass extraction and slow washout in the kidneys. The goal of this study was to investigate the feasibility of human kidney imaging with ⁸²Rb positron emission tomography (PET) and obtain quantitative data of its uptake non-invasively.

Methods: Eight healthy volunteers underwent dynamic PET/CT imaging with ⁸²Rb. A preprogrammed pump was used to insure reproducible injections. Tissue time activity curves were generated from the renal cortex. An input function was derived from the left ventricular blood pool (LVBP), the descending thoracic aorta and the abdominal aorta. Renal blood flow was estimated by applying a two-compartment kinetic model. Results obtained with different input functions were compared.

Results: Radiotracer accumulation was rapid and reached a plateau within 15–30 s after the bolus entered the kidneys. The derived K1 and k2 parameters were reproducible using input functions obtained from diverse vascular locations. K1 averaged 1.98 ± 0.14 mL/min/g. The average k2 was 0.35 ± 0.11 /min. Correlation between K1 values obtained from the LVBP from different bed positions when the kidneys and abdominal aorta were in the same field of view was excellent ($R = 0.95$).

Conclusions: Non-invasive quantitative human kidney imaging with ⁸²Rb PET is feasible. Advantages of renal PET with ⁸²Rb include excellent image quality with high image resolution and contrast. ⁸²Rb has potential as a clinical renal imaging agent in humans.

Key words: compartmental model; renal blood flow; renal PET/CT; Rubidium-82 chloride.

Introduction

Positron emission tomography (PET) using [¹⁸F] fluoro-2-deoxy-D-glucose (FDG) has been established as an important clinical tool, particularly in oncology. FDG PET is now routinely used in the detection, staging, evaluation of treatment response and prognosis in various cancers.^{1,2} The use of PET to address questions in cardiology is growing rapidly. Oxygen-15 water, Nitrogen-13 ammonia and Rubidium-82 are perfusion tracers commonly employed with PET for the non-invasive assessment of myocardial blood flow (MBF) in individuals with suspected or known cardiac disease.^{3–5}

The development of clinical PET imaging of the kidneys has been slow, partly due to the success of single photon

renal imaging, with both planar and SPECT, and the usefulness of other non-invasive imaging modalities such as ultrasound, MR angiography and CT angiography.

Radiopharmaceuticals tagged with positron-emitting radionuclides such as ¹⁵O-water, ¹³N-ammonia, Rubidium-82 chloride (⁸²Rb) and ⁶²Cu-PTSM have been used for more than two decades mainly as perfusion agents in animal models.^{6,7} Tracers used for perfusion imaging fall into two categories: category I tracers such as ¹⁵O-labeled water are freely diffusible between tissue and blood; category II tracers such as ⁸²Rb, ¹³N-ammonia and ⁶²Cu-PTSM are physiologically retained in the tissue.^{7,8} To our knowledge human imaging studies of the kidneys with ⁸²Rb have not yet been published.

^{82}Rb is a potassium analogue with an ultra short half-life of 75 s and a maximum positron energy of 3.35 MeV. It demonstrates high first pass extraction in the kidneys in animal models. There is a close correlation between measurements of renal blood flow with ^{82}Rb and microspheres in canine kidneys.⁹ Renal blood flow (RBF) measured by ^{82}Rb PET showed a significant decrease from baseline after acute unilateral renal artery stenosis and intravenous injection of captopril in instrumented dogs, underscoring its potential as a perfusion tracer for evaluation of pathologic renal conditions.^{10,11}

^{82}Rb is commercially available from $^{82}\text{Sr}/^{82}\text{Rb}$ generator, appears to possess suitable kinetics for renal imaging based on preclinical data and is widely used for myocardial perfusion studies in humans.⁵ ^{82}Rb PET imaging of the kidneys has potential for clinical utilization.

The goal of this preliminary study was to investigate the feasibility of human kidney imaging with ^{82}Rb PET and to obtain the first quantitative data on its renal uptake non-invasively.

Methods

Dynamic scans from eight healthy volunteers (four male and four female, age 31.0 ± 9.0 years), all with normal renal function (Cre 0.86 ± 0.16 mg/dL, GFR > 60 mL/min) who underwent dynamic PET/CT imaging as part of a Human Biodistribution and Radiation Dosimetry study of ^{82}Rb ¹² were included. That study had 10 volunteers; however, in two subjects the input from the abdominal aorta could not be defined unambiguously and were not included in the present study. The details of the image acquisition protocol have been described.¹² In short, immediately after intravenous bolus injection of 536 ± 100 MBq of ^{82}Rb Chloride, PET was performed in list mode for 8 min per bed position. Six contiguous single-bed positions were completed for each subject lying in the supine position. OSEM reconstruction (21 subsets, 2 iterations) was applied to decay corrected dynamic sequences, with 32 frames (20×6 s, 5×12 s, 4×30 s and 3×60 s). Corrections for attenuation, normalization, randoms, scatter and dead time were also included. A phantom study was performed to directly cross-calibrate the PET/CT scanner with the ^{82}Rb generator infusion system.

In three subjects, both the left ventricular blood pool and the kidneys were included in the same acquisition. In five patients, the kidneys and the left ventricle appeared in two different acquisitions. The tracer injection was accomplished using a preprogrammed pump that delivered reproducible injections.

PET images from table positions that included the heart and the kidneys were imported into *DynamicPET* software on a GE Xeleris workstation (General Electrical, Milwaukee, WI, USA). Time activity curves (TACs) were generated by placing regions of interest (ROI) on the left ventricular cavity, descending thoracic aorta, abdominal

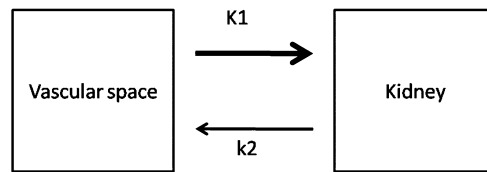


Fig. 1. Two-compartment model used for kinetic modeling of ^{82}Rb in the kidneys and for parameter estimation. The input function representing the vascular compartment was derived from the left ventricular cavity, the thoracic aorta or the abdominal aorta. K1 represents tracer uptake e.g. renal blood flow \times extraction fraction. k2 represents tracer release from the kidneys back to the vascular space. No discernible tracer excretion was observed in the renal collecting system during the time of PET imaging of 8 min.

aorta and kidneys. All images were corrected for attenuation and TACs were also corrected for radionuclide decay.

A two-compartment model was applied for quantitative evaluation of tracer kinetics and estimation of RBF. This was deemed appropriate since no urinary excretion was noted during the time of dynamic acquisition. Compartmental modelling was accomplished using a Matlab-based in-house software, which had been previously validated against the PMOD software (PMOD Technologies Ltd, Zurich, Switzerland) and has extensively been used in a number of ^{82}Rb myocardial perfusion studies.^{13,14}

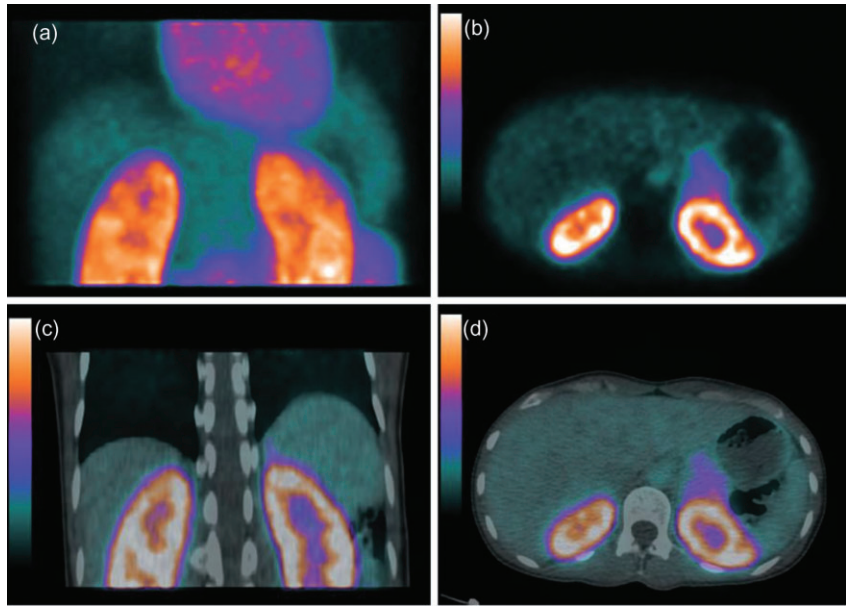
Figure 1 depicts the two-compartment model and the definition of the parameters used. A blood volume term was also modelled to account for presence of signal from the blood compartment within the kidney ROIs. Constrained least-squares minimization was applied for parameter estimation, restricting K1, k2 and the blood volume to be non-negative. Values for the parameters were obtained for various input functions including the left ventricular blood pool, the descending thoracic aorta, and the abdominal aorta. The K1 parameter was used for estimation of RBF. As a first approximation of partial volume correction, TACs from the thoracic and abdominal aortas were rescaled to match maximum activity of the TAC obtained from the left ventricle. Results obtained with different input functions were compared.

Results

^{82}Rb demonstrated high uptake in the kidneys which resulted in excellent image quality (Fig. 2). Tracer accumulation in the kidneys was much higher than in the myocardium. The TACs showed that activity in the kidneys was greater by a factor of 4 as compared with the myocardium and by a factor of 10 as compared with left ventricular blood pool (Fig. 3). The renal cortex was delineated but the medulla could not be clearly seen or separated from the renal pelvis.

The input functions derived from the ascending thoracic aorta, the descending thoracic aorta and the abdominal aorta acquired in the same bed position as the

Fig. 2. MIP (a), transaxial PET (b), coronal fused PET/CT (c) and transaxial fused PET/CT (d) images from a study where the kidneys and the heart appeared in the same field of view. The images represent the time integral of the entire PET study of 8 min.



left ventricle and from the abdominal aorta obtained in a different bed position were comparable. They were also comparable to left ventricular blood pool activity after they were scaled to the maximum (Fig. 4). The reproducibility for different bed positions was achieved by automated injections of ^{82}Rb . Tissue accumulation was rapid and reached a plateau within 1 min after the bolus first reached the kidneys.

The compartmental curve fit of the renal cortical TAC was very reasonable and residual analysis confirmed the appropriateness of the two-compartment (blood pool + tissue) model (Fig. 5).

The estimated values of both K_1 and k_2 were symmetrical between the right and left kidneys in the same individual and the values were also comparable between subjects and between different input functions applied

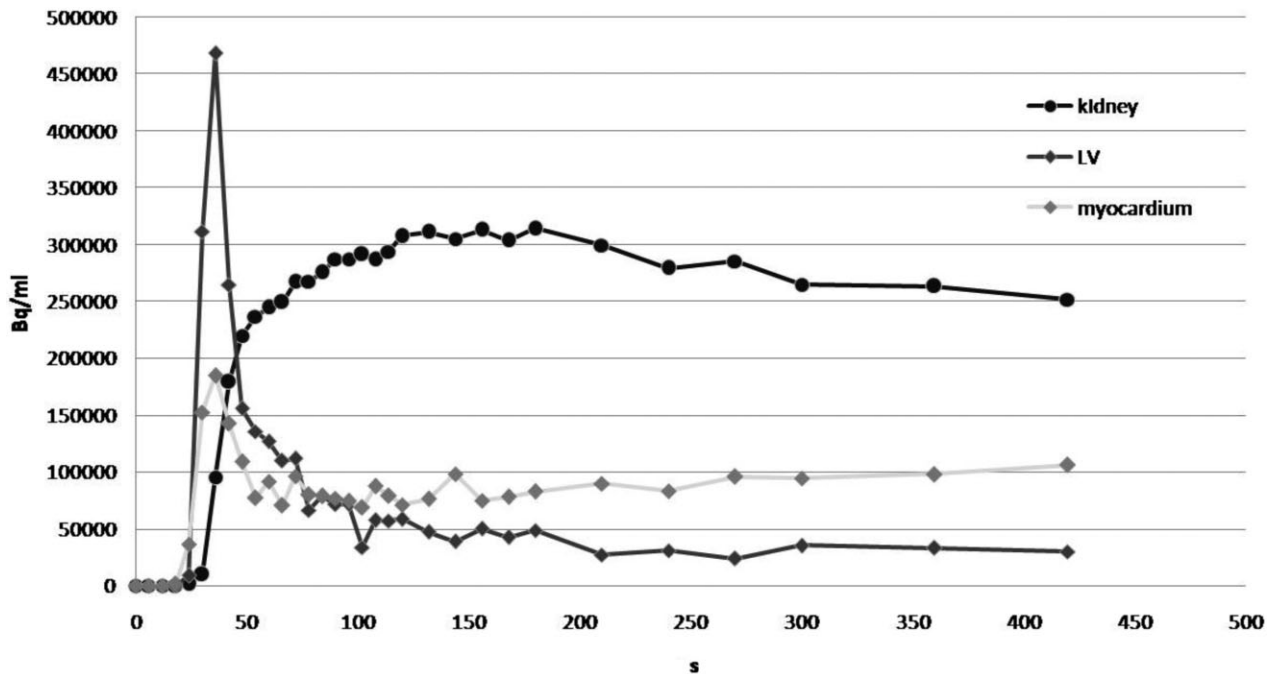


Fig. 3. Time activity curves obtained from the left ventricular blood pool, myocardium and kidneys from one subject. Activity and uptake in the kidneys is greater by about a factor of 4 as compared with the myocardium.

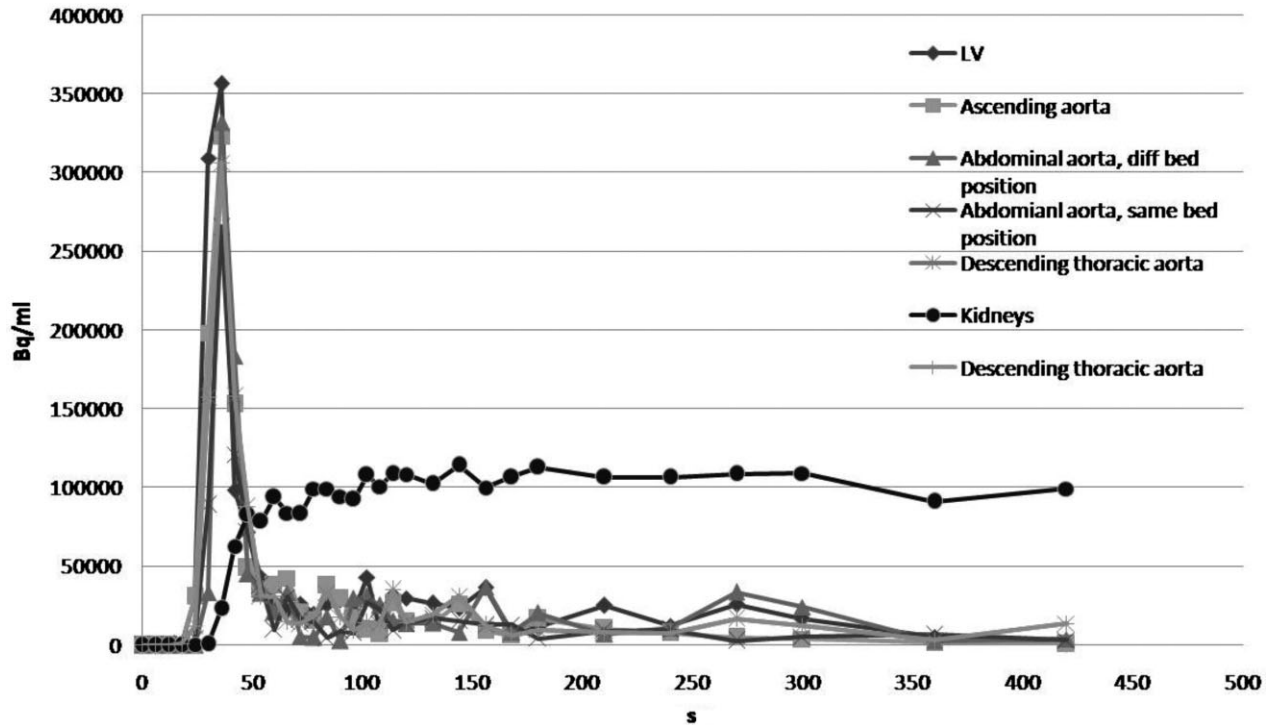


Fig. 4. Time activity curves from the kidneys and vascular input functions derived from the left ventricular blood pool, ascending and descending thoracic aortas, and the abdominal aorta. In this subject the kidneys and the heart were imaged in different bed positions.

for fitting (Table 1). In subject 1 and subject 7, reproducible parameters were observed both with the input function derived from left ventricular in the same and different bed position as the kidneys. For both these patients, the left ventricle appeared partially in two bed positions.

Table 2 shows average K1 values estimated for five different input functions from the left ventricle (in different or same bed position as the kidneys), descending thoracic aorta and the abdominal aorta. Right and left kidney values were averaged for each patient. The K1 values from different input functions correlate well with one another. Specifically, the K1 values obtained abdominal aorta versus left ventricle (including both results from the same and different bed positions) demonstrated high correlation ($r = 0.97$).

As a measure of reproducibility, the intra-class correlation coefficient (ICC)¹⁵ for the individual right versus left kidney measurements was calculated and showed high reproducibility with ICC values of 0.98, 0.92, 0.99, 0.95 and 0.99, respectively, for the above-mentioned five different input functions.

Discussion

This study illustrates that imaging of kidneys and non-invasive quantification of RBF is feasible in humans using ⁸²Rb PET.

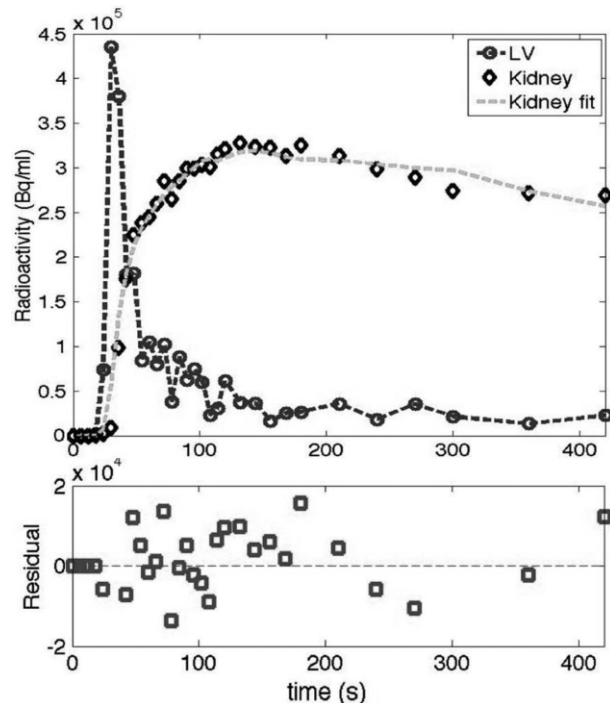


Fig. 5. Typical results from compartmental curve-fitting using validated in-house software. The top depicts raw data points from vascular input functions and tissue curves from the kidneys, including the fitted curve. The bottom of the figure shows the residuals from the compartmental fitting.

Table 1. Compartmental model parameters for all eight healthy volunteer subjects using different input functions

		K1 (mL/min/g)		k2 (1/min)	
		Right	Left	Right	Left
Subject 1	LV diff	1.90	1.91	0.20	0.20
	LV same	1.91	1.91	0.26	0.26
	TA same	2.14	2.18	0.29	0.28
	AA same	2.18	2.22	0.25	0.24
Subject 2	LV diff	2.01	2.13	0.27	0.28
	TA diff	2.29	2.43	0.22	0.23
	AA same	2.25	2.39	0.27	0.28
Subject 3	LV diff	1.78	1.66	0.19	0.17
	TA diff	1.75	1.63	0.20	0.17
	AA same	1.74	1.61	0.28	0.25
Subject 4	LV diff	1.17	1.13	0.15	0.16
	TA diff	1.22	1.18	0.12	0.13
	AA same	1.35	1.30	0.12	0.12
Subject 5	LV same	2.07	2.09	0.49	0.47
	TA same	1.92	1.93	0.28	0.27
	AA same	2.54	2.55	0.29	0.27
Subject 6	LV diff	1.62	1.68	0.23	0.23
	TA diff	1.78	1.85	0.20	0.21
	AA same	1.84	1.91	0.25	0.25
Subject 7	LV diff	2.00	1.92	0.39	0.35
	LV same	2.13	2.05	0.34	0.32
	TA same	2.17	2.09	0.24	0.21
	AA same	2.49	2.40	0.41	0.38
Subject 8	LV diff	2.07	2.14	0.20	0.22
	TA diff	1.99	2.07	0.16	0.17
	AA same	2.51	2.60	0.29	0.31

AA, abdominal aorta at the kidney level; diff, different table position from kidneys; LV, left ventricle; same, same table position as kidneys; TA, descending thoracic aorta.

The dose of ^{82}Rb used in these studies was about half of that usually injected for cardiac PET studies (536 ± 100 MBq). Nonetheless, the image quality in all subjects was excellent, with very high cortical-to-background ratios and no noticeable tracer excretion into the collecting system. Accumulation was rapid and reached a plateau within 15–30 s after the bolus reached the

Table 2. Average values of the K1 parameter from both kidneys using different input functions

Input function	n	K1 (mL/min/g)	
		Mean	STD
LV diff	7	1.793	0.329
LV same	3	2.028	0.101
TA same	3	1.819	0.430
TA diff	5	2.071	0.126
AA same	8	2.117	0.449

AA, abdominal aorta at the kidney level; diff, different table position from kidneys; LV, left ventricle; same, same table position as the kidneys; TA, descending thoracic aorta.

kidneys. The uptake and accumulation in the kidneys was higher by a factor of 4 to 5 as compared with the myocardium.

An advantage of ^{82}Rb is its availability from commercial $^{82}\text{Sr}/^{82}\text{Rb}$ generators. Its independence from an onsite cyclotron makes it an ideal tracer for organ perfusion measurements in community PET/CT centres. ^{82}Rb is already widely used as a cardiac PET agent to assess myocardial flow and flow reserve in coronary artery diseases.^{5,16} ^{82}Rb also has potential to become a renal PET tracer as the uptake in the renal cortex is much higher than in the myocardium.

The current study shows good reproducibility of the compartmental model parameters, especially of the tracer uptake coefficient K1 even with input functions obtained from different injections and bed positions. Future work will require determination of the relationship between RBF and the perfusion coefficient K1, as existing data in the literature are very limited.

In a preclinical renal study with dogs using ^{82}Rb ,⁹ an average extraction rate of 0.89 was calculated. However, using that value and a mean value for K1 of 1.9 mL/cc/min obtained from healthy subjects in the present work, we would obtain a mean blood flow of 2.2 mL/min/g. Using an average human kidney size of about 150–200 g,¹⁷ the estimated RBF with ^{82}Rb is 330–440 mL/min per kidney, or 660–880 mL/min for both kidneys, which is underestimated compared with previously accepted values of 1000–1100 mL/min using dynamic CT,¹⁸ or hematocrit corrected para-aminohippurate clearance.¹⁹ In previous studies, the extraction coefficients⁹ were quantified using non-tomographic beta probes rather than PET imaging and showed increasing extraction values with increasing flow.

Hypothetically, one could utilize the experience already obtained from MBF determinations with ^{82}Rb and consider the generalized Renkin–Crone formulation for the extraction fraction E as a function of flow F :

$$E = \left(1 - ae^{-\frac{b}{F}}\right); K_1 = E \cdot F \quad (1)$$

Using radiolabelled microspheres for validation of ^{82}Rb myocardial perfusion in dogs, Yoshida *et al.*²⁰ and Lautamaki *et al.*²¹ estimated (a, b) values of (0.85, 0.45) and (0.89, 0.68), respectively. Lortie *et al.*,²² on the other hand, calculated values of (0.77, 0.63), but that work utilized ^{13}N -ammonia PET scans as reference. Considering the fact that K1 values estimated from ^{13}N -ammonia themselves need to be compensated for extraction, which can be achieved using relations obtained in previous works,^{20,23} all above-mentioned conversions result in comparable regressions between ^{82}Rb K1 and MBF. In the present work the mean K1 values were ~ 1.9 mL/min/g in healthy subjects, which corresponds to an extraction fraction of $<19\%$, resulting in significant underestimation of RBF by the K1.

In the work by Chen *et al.*,²⁴ ¹³N-ammonia PET studies were performed in dogs and compared to microsphere studies. A different model for the calculation of the extraction fraction was utilized involving the retention fraction E_r leading to:

$$E_r = \left(1 - ae^{-\frac{b}{F}}\right); K_1 = \frac{E_r}{1 - E_r} \cdot F \quad (2)$$

wherein (a, b) were determined to be (0.83, 1.35). In the normal RBF range relevant to the present work, the extraction fraction would be 50–60%, which is a more reasonable estimate compared with the above-mentioned over- and underestimated extraction fractions. In any case, for renal PET imaging using ⁸²Rb, clearly an appropriate calibration method is needed to better relate the parameter K1 of the compartment model to absolute RBF for ⁸²Rb. In humans, this calibration could be achieved using ¹⁵O-H₂O PET. In experimental animals, more invasive techniques such as radioactive microspheres or arterial and venous sampling could be implemented. This suggests future directions subsequent to the present feasibility study.

Another important consideration to achieve truly quantitative imaging in the proposed context is the fact that even though the various input functions were shown to yield highly correlated K1 values, differences up to 10–20% in the actual values were observed. This observation emphasizes the potential need for development and implementation of accurate partial volume correction in the present context.²⁵ An additional limitation of this study is the lack of patient data. Once a rigorous calibration method is obtained that relates the kinetic parameter K1 to RBF, additional studies with patients are needed to better elucidate the clinical value of PET imaging using ⁸²Rb once these issues are addressed. Particular applications could include renovascular disease, acute tubular necrosis (pre- and post-therapy), and acute and chronic transplant nephropathy, e.g. situations where diagnostic functional imaging is required but applicability of MRI or CTA contrast agents is limited by their potential toxicity in patients with limited kidney function.

Conclusion

The present study shows that renal PET with ⁸²Rb yields excellent image quality with high resolution and delineation of the renal cortex with low background activity. Usage of different approaches to estimate the input function was investigated, and these approaches yielded reasonable reproducibility and consistency. ⁸²Rb is demonstrated as having potential as a clinical renal imaging agent in humans. However, for appropriate quantification, it is necessary to establish the flow-dependent extraction of the radiopharmaceutical in the kidneys. Once a rigorous calibration method is obtained that relates the kinetic parameter K1 to RBF, additional

studies with patients are needed to better elucidate the clinical value of PET imaging using ⁸²Rb.

Acknowledgements

The human ⁸²Rb dosimetry study was supported by a research grant from Bracco Diagnostics Inc. (Princeton, NJ).

References

- Weber WA. Use of PET for monitoring cancer therapy and for predicting outcome. *J Nucl Med* 2005; **46**: 983–95.
- Wahl RL, Zasadny K, Helvie M, Hutchins GD, Weber B, Cody R. Metabolic monitoring of breast cancer chemohormonotherapy using positron emission tomography: initial evaluation. *J Clin Oncol* 1993; **11**: 2101–11.
- Tamaki N, Yonekura Y, Senda M *et al.* Myocardial positron computed tomography with ¹³N-ammonia at rest and during exercise. *Eur J Nucl Med* 1985; **11**: 246–51.
- Schelbert HR, Phelps ME, Huang SC *et al.* N-13 ammonia as an indicator of myocardial blood flow. *Circulation* 1981; **63**: 1259–72.
- Bengel FM, Higuchi T, Javadi MS, Lautamäki R. Cardiac positron emission tomography. *J Am Coll Cardiol* 2009; **54**: 1–15.
- Alpert NM, Rabito CA, Correia DJ *et al.* Mapping of local renal blood flow with PET and H(2)(15)O. *J Nucl Med* 2002; **43**: 470–75.
- Szabo Z, Xia J, Mathews WB, Brown PR. Future direction of renal positron emission tomography. *Semin Nucl Med* 2006; **36**: 36–50.
- Hutchins GD. What is the best approach to quantify myocardial blood flow with pet? *J Nucl Med* 2001; **42**: 1183–4.
- Mullani NA, Ekas RD, Marani S, Kim EE, Gould KL. Feasibility of measuring first pass extraction and flow with rubidium-82 in the kidneys. *Am J Physiol Imaging* 1990; **5**: 133–40.
- Tamaki N, Rabito CA, Alpert NM *et al.* Serial analysis of renal blood flow by positron tomography with rubidium-82. *Am J Physiol* 1986; **251** (5 Pt 2): H1024–30.
- Tamaki N, Alpert NM, Rabito CA, Barlai-Kovach M, Correia JA, Strauss HW. The effect of captopril on renal blood flow in renal artery stenosis assessed by positron tomography with rubidium-82. *Hypertension* 1988; **11**: 217–22.
- Senthamizhchelvan S, Bravo PE, Esaias C *et al.* Human biodistribution and radiation dosimetry of ⁸²Rb. *J Nucl Med* 2010; **51**: 1592–9.
- Tang J, Bengel F, Rahmim A. Cardiac motion-corrected quantitative dynamic Rb-82 PET imaging. *J Nucl Med* 2010; **51** (Suppl 2): 123.
- Tang J, Rahmim A, Lautamaki R, Lodge MA, Bengel FM, Tsui BM. Optimized regional myocardial blood

- flow abnormality detection in dynamic Rb-82 PET. *J Nucl Med* 2009; **50** (Suppl 2): 467.
15. Shrout PE, Fleiss JL. Intraclass correlations – uses in assessing rater reliability. *Psychol Bull* 1979; **86**: 420–28.
 16. Di Carli MF, Dorbala S, Meserve J, El Fakhri G, Sitek A, Moore SC. Clinical myocardial perfusion PET/CT. *J Nucl Med* 2007; **48**: 783–93.
 17. Vasconcelos VT, Katayama RC, Ribeiro MF, Medina-Pestana JO, Baptista-Silva JC. Kidney weight and volume among living donors in Brazil. *Sao Paulo Med J* 2007; **125**: 223–5.
 18. Miles KA. Measurement of tissue perfusion by dynamic computed tomography. *Br J Radiol* 1991; **64**: 409–12.
 19. Splenser AE, Fisher ND, Danser AH, Hollenberg NK. Renal plasma flow: glomerular filtration rate relationships in man during direct renin inhibition with aliskiren. *J Am Soc Hypertens* 2009; **3**: 315–20.
 20. Yoshida K, Mullani N, Gould KL. Coronary flow and flow reserve by PET simplified for clinical applications using rubidium-82 or nitrogen-13-ammonia. *J Nucl Med* 1996; **37**: 1701–12.
 21. Lautamaki R, George RT, Kitagawa K *et al.* Rubidium-82 PET-CT for quantitative assessment of myocardial blood flow: validation in a canine model of coronary artery stenosis. *Anglais* 2009; **36**: 576–86.
 22. Lortie M, Beanlands RS, Yoshinaga K, Klein R, Dasilva JN, DeKemp RA. Quantification of myocardial blood flow with 82Rb dynamic PET imaging. *Eur J Nucl Med Mol Imaging* 2007; **34**: 1765–74.
 23. Bellina CR, Parodi O, Camici P *et al.* Simultaneous in vitro and in vivo validation of nitrogen-13-ammonia for the assessment of regional myocardial blood flow. *J Nucl Med* 1990; **31**: 1335–43.
 24. Chen BC, Germano G, Huang SC *et al.* A new noninvasive quantification of renal blood-flow with N-13 ammonia, dynamic positron emission tomography, and a 2-compartment model. *J Am Soc Nephrol* 1992; **3**: 1295–306.
 25. Rousset O, Rahmim A, Alavi A, Zaidi H. Partial volume correction strategies in PET. *PET Clin* 2007; **2**: 235–49.